Semiconductor Optical Amplifiers with Low Noise Figure

*Hideaki Hasegawa *, Masaki Funabashi *, Kazuomi Maruyama *,*
*Kazuaki Kiyota *, and Noriyuki Yokouchi **

ABSTRACT In the multilevel phase modulation which is expected to provide the next-generation modulation format for optical communications, the insertion losses of the optical transmitters and receivers tend to increase due to their structural complexity with advancement in the modulation level. For this reason, there is a need for a compact single-channel optical amplifier to compensate for such insertion losses, and a semiconductor optical amplifier (SOA), which is smaller than an erbium doped fiber amplifier (EDFA) and capable of being integrated with other optical devices is drawing the attention for such applications. In this study, the design of SOA structures was optimized using simulation techniques, and prototypes were fabricated. The prototyped SOA has an output power of 5 dBm or higher and a noise figure (NF) of 4 dB or lower at 100 mA of current satisfying the requirements for a single-channel optical amplifier, whose characteristics are similar to those of an EDFA, and thus, holds a considerable promise as an optical amplifier of compact size, low power consumption and low noise.

1. INTRODUCTION

Multilevel phase modulation schemes, which are based typically on phase shift keying (PSK), are drawing attention as a next-generation optical communication method for their superiority to conventional on-off keying (OOK) schemes in terms of receiver sensitivity, spectrum efficiency and dispersion tolerance characteristics. However, the insertion losses of the optical transmitters and receivers tend to increase as the modulation level advances because of the increasing number of optical components as the modulation system uses multistage phase modulators on the transmitter side and passive delay circuits and balanced photodetectors on the receiver side. Figure 1 shows the schematic structure of a modulator for a 16 quadrature amplitude modulation (16QAM) using four sets of Mach-Zehnder interferometers, which results in a high insertion loss of about 10 dB [1]. Compact SOAs are recently drawing attention to compensate for such high insertion losses. The SOAs can be integrated either monolithically with other compound semiconductor-based optical devices, or in a hybrid manner with silica-based optical waveguides of planar lightwave circuits (PLCs) with a low coupling loss of below 1 dB by using a spot size converter (SSC) [2]. Moreover, the SOAs have many advantages such as simple current pumping, compactness, low power consumption and low cost. In order to be used as a single channel amplifier for optical communications, on the other hand, the SOAs are required to provide a polarization-insensitive gain and a low NF, which are similar to those of an EDFA. The aim of this study is to satisfy the SOA characteristics of both low noise and high output, making it possible to develop an SOA which satisfies the required characteristics for a single-channel amplifier. SOAs with low noise figure and high output characteristics have already been reported in the literature [3]. But this paper has not described the dependence of NF on structural parameters such as the active layer width, the gain region length and the active layer structure with the multi quantum well (MQW). Accordingly in this study, we carefully investigated numerically, as well as experimentally, the dependence of NF on the active layer width, on the gain region length and on the active layer structure. Furthermore, we optimized the active layer width and the gain region length to realize SOA characteristics that meet the NF and the output power requirements for a typical single-channel amplifier.

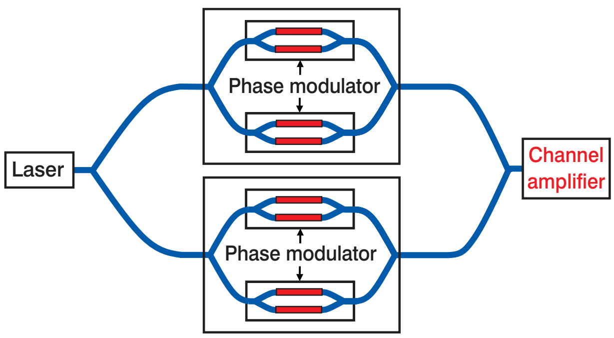

Figure 1 **Schematic structure of the 16QAM modulator.**

* Photonic Device Research Center, Yokohama R&D Lab. R&D Div.

2. ANALYSIS TECHNIQUES FOR SOA CHARACTERISTICS

Analysis techniques for the NF and output power characteristics of an SOA will be described in this section. The analysis technique for the NF characteristics of an SOA is introduced in the literature [4]. The fundamental equation used in this analysis is a rate equation describing the temporal changes of carrier density as shown in Equation (1).

$$\frac{dN(z,t)}{dt}=\frac{I}{eN_{QW}dWL}-R(N(z,t))-\frac{\Gamma}{N_{QW}dW}g(N)[Q_k^+(z,t)+Q_k^-(z,t)]$$
$$-\frac{2\Gamma}{N_{QW}dW}g(N)K[Q_j^+(z,t)+Q_j^-(z,t)] \quad (1)$$

where

$N(z,t)$	carrier density;
I	electric current;
e	charge amount;
d	thickness of a quantum well layer;
N_{QW}	number of quantum wells;
W	width of active layer;
L	gain region length of SOA;
K	coefficient representing the multiplicity of end facet reflection;
$R(N(z,t))$	recombination rate term;
Γ	optical confinement factor;
$g(N)$	material gain coefficient;
$Q_k^+(z,t)$, $Q_k^-(z,t)$	photon density of forward and backward propagating signal lights, respectively;
$Q_j^+(z,t)$, $Q_j^-(z,t)$	photon density of forward and backward propagating amplified spontaneous emissions (ASE), respectively.

By solving this rate equation and the propagation equations of the signal light and ASE light simultaneously, the distribution of the signal light and ASE light can be obtained. Letting G be the gain, CE be the coupling efficiency on the receiving side and P_{ASE} be the intensity of the ASE at the output, the noise figure NF (dB) can be calculated from the following equation:

$$NF(\mathrm{dB})=10\log_{10}\left(\frac{2P_{ASE}(\nu)}{h\nu\Delta\nu G(\nu)}+\frac{1}{G(\nu)}\right)\cdot CE \quad (2)$$

From Equation (2), it can be seen that the NF is determined mainly by the gain G and the power of ASE light.

In case of the laser analysis, the material gain coefficient $g(N)$ in Equation (1) is expressed by an approximated model shown in Equation (3).

$$g(N)=g_0 ln(N/N_0) \quad (3)$$

By substituting the approximated model shown in Equation (3) into Equation (1), the characteristic analysis of an MQW SOA can be carried out. In Equation (3), g_0 is the gain coefficient, N is the carrier density and N_0 is the transparency carrier density. Figure 2 compares the net gain calculated by the approximated model and the one measured by using the Hakki-Paoli method. The net gain G_{net} can be expressed by Equation (4).

$$G_{net}(N)=\Gamma g(N)-\alpha(N) \quad (4)$$

where $\alpha(N)$ is the loss.

Whereas, as shown in Figure 2, the approximated model by Equation (3) suggests a tendency for the net gain to rise as the injected carrier density increases, the measured net gain tends to rapidly saturate on the high-carrier density side. While lasers operate at low-carrier density due to carrier clamping, SOAs come to operate at high-carrier density, so that the net gain at high-carrier density becomes important. In this study, considering that the model based on Equation (3) cannot accurately express the material gain at high carrier concentration, the measured net gains were used in the analysis. Figure 3 shows the gain and NF characteristics calculated using the approximated model and those calculated using actual measurement data. It can be seen that, while the approximated model gives differences from experimental results of 4.1 dB and 0.7 dB for the gain and NF, respectively, those differences are reduced to 1.2 dB and 0.2 dB respectively by using the measured net gain for calculation.

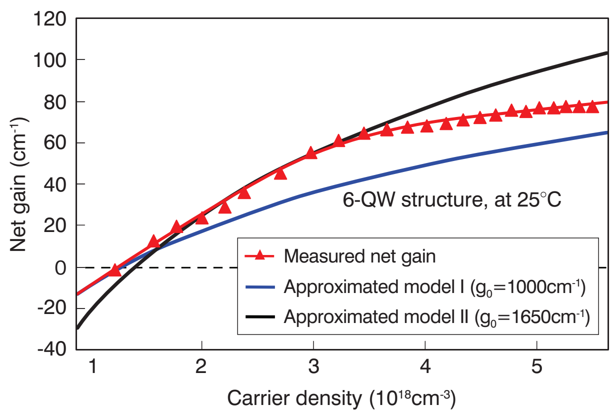

Figure 2 Comparison of calculated net gains using approximated model and measured values.

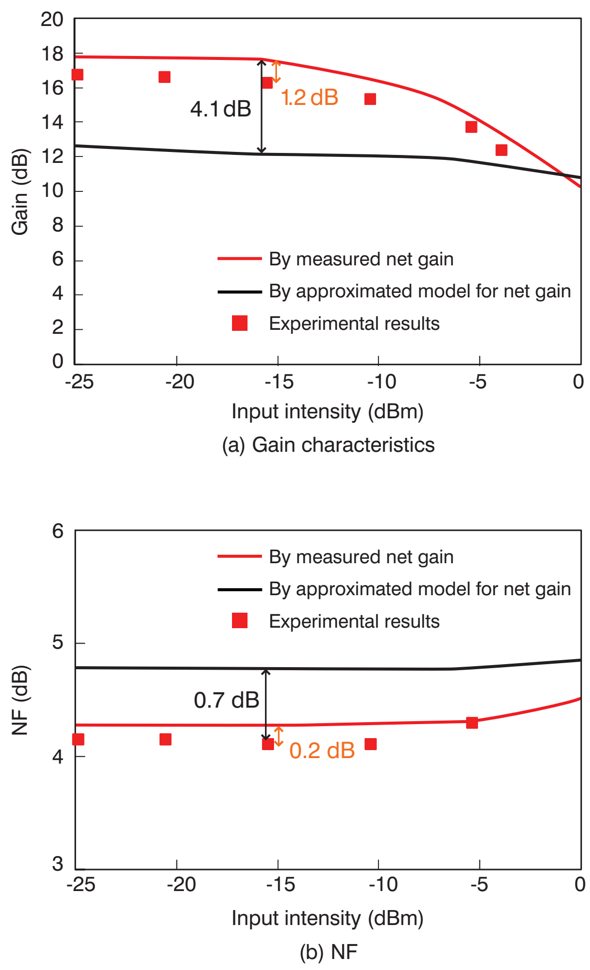

Figure 3 Experimental results and calculated results for gain (a), and NF (b), using net gains based on approximated model and measurement.

3. DESIGN OF LOW NOISE SOA

The waveguide structures of low-noise SOAs have been designed using the analysis techniques described above. Figure 4 illustrates the structure parameters of an SOA considered for the design. Structure parameters to be designed include the active layer width W, the gain region length L, the optical confinement factor Γ and the loss α. The device fabricated here uses an active layer of GaInAsP, and employs buried hetero-structure for the waveguide. Figure 5 shows the relationship between the active layer W and gain region length L at a pumping current of 100 mA and input power of -5 dBm for a device consisting of three active layers (3-QW) and having an optical confinement factor Γ of 1.1%. From Figure 5, the noise figure is seen to decrease as the active layer width increases and the gain region length shortens. It is also reported that NF decreases as optical confinement factor and loss decline [6]. In other words, the NF tends to decrease with the wider active layer, with the shorter gain region length, with the lower loss and with the lower optical confinement factor. Figure 6 shows the calculated results of the signal light distribution along the propagation direction in SOAs having different optical confinement factors. It is seen from the figure that the lower the optical confinement factor, the more resistant to saturation is the signal light along the longitudinal direction, and the lower the NF tends to be. In such a structure, since the gain saturation of signal light is less likely to occur, injected carriers are transformed more into signal light than into noise light, so that the NF tends to decrease. Consequently, to realize low-noise characteristics it is important to design a waveguide structure in which the signal light is less susceptible to saturation. The blue solid line in Figure 5 (a) and (b) shows the targeted performance of 5 dBm and 4 dB for the optical output power and chip NF, respectively; and the red solid line at 2.8 μm shows the boundary for satisfying the condition for single mode operation. In fact, we have fabricated prototype SOAs with a waveguide structure that meet the targeted optical output power, the NF and the single-mode conditions, by setting the active layer width to 2.8 μm and gain region length to 1000 μm.

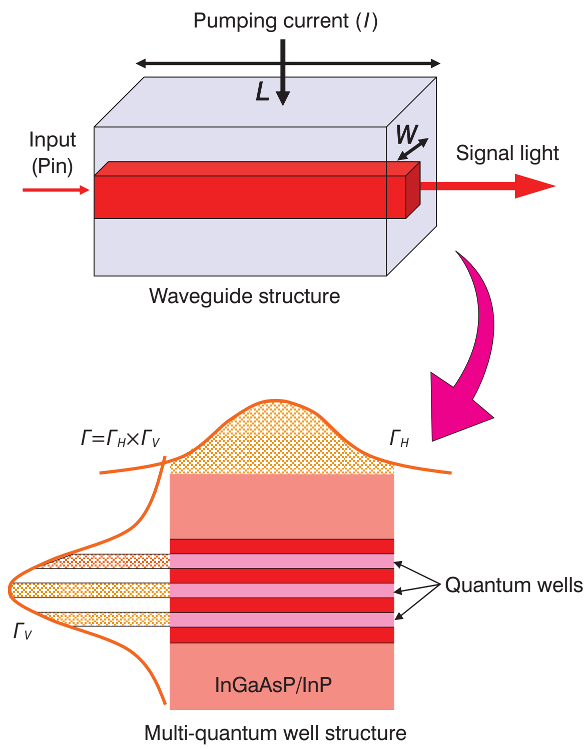

Figure 4 Structure parameters of the SOA.

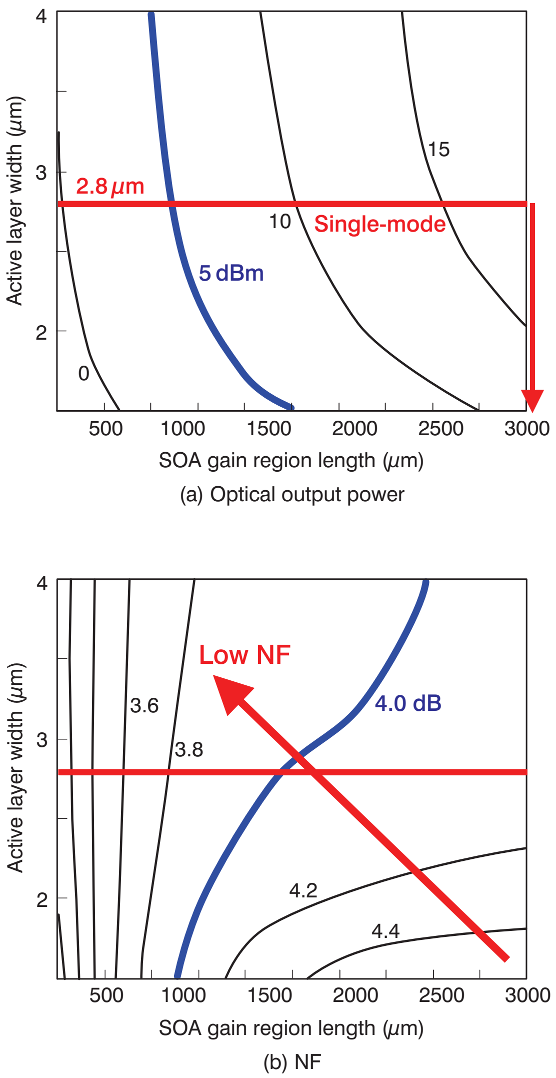

Figure 5 **The output power (a) and the NF (b), depending on an active layer width and a gain region length.**

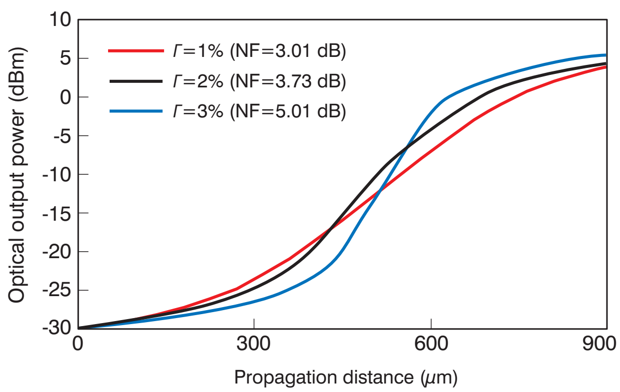

Figure 6 **The signal light distribution in SOAs with different optical confinement factors.**

4. FABRICATION OF PROTOTYPE LOW NOISE SOA

Prototypes were fabricated in accordance with the waveguide structure design described in Section 3, and in addition, the number of quantum wells was increased in turn from the predetermined value of three (3-QW) to five (5-QW) and eight (8-QW). Metal organic chemical vapor deposition (MOCVD) was used for crystal growth, and the active layer is made up of GaInAsP quantum wells with a 0.8% compressive strain. Buried heterostructure was used for current confinement, and multistep separate confinement heterostructure (SCH) was employed to reduce the optical absorption at the p-doped upper cladding layer. Further, anti-reflection coating was applied to the end facets. Figure 7 shows the optical output power and the NF characteristics of the 3-QW, 5-QW, and 8-QW SOAs prototyped here. Bench-top measurements were conducted using an automatic fiber alignment system. The measurement wavelengths were set to 1500 nm, 1560 nm and 1560 nm, corresponding to the peak gain wavelength of 3-QW, 5-QW, and 8-QW device, respectively. In the figure, the ■, ● and ▲ plots represent the measured optical output power and the NF of a 3-QW, a 5-QW, and a 8-QW, respectively. The solid line represents the calculated results. In the calculation, the Γ values obtained by the mode analysis are used, and they are 1.1%, 2.3% and 4.4% for the 3-QW, the 5-QW, and the 8-QW, respectively. In terms of loss, the absorption loss at the active layer is dominant since the SOAs operate under the pumping conditions of a high carrier density, and the absorption loss at the active layer is known to be proportional to Γ [7]. The loss for the 3-QW structure is 8 cm^{-1}, which is a measured value, and those for the 5-QW and 8-QW structures are 17 cm^{-1} and 32 cm^{-1}, respectively, which are estimated values assuming a proportional relationship to Γ. The experimental results show that the 3-QW and the 5-QW structures have almost the same NF. Increasing the number of wells produces two effects: one is that since the operating carrier density decreases the gain become less likely to saturate, so that the NF decreases--which is referred to as "effect A"; and the other is that the absorption loss in the active layer increases, thus increasing the NF--"effect B". It is considered that, for the 3-QW and the 5-QW structures, these two effects cancel each other, so that the NF shows virtually no change. On the other hand, since the effect B becomes dominant in the case of the 8-QW, the NF rapidly increases. In terms of output power, it is thought that since the net gain increases in proportion to Γ as the number of wells increases from 3-QW to 5-QW and to 8-QW, the output power is high at the low-input power side of below -5 dBm, but it decreases due to gain saturation at the high-input power side. It can also be seen that, among the three active layer structures prototyped here, the 5-QW satisfies both the output power and the NF at an optical input power of below -5 dBm that is assumed to be the operating condition for a single-channel amplifier.

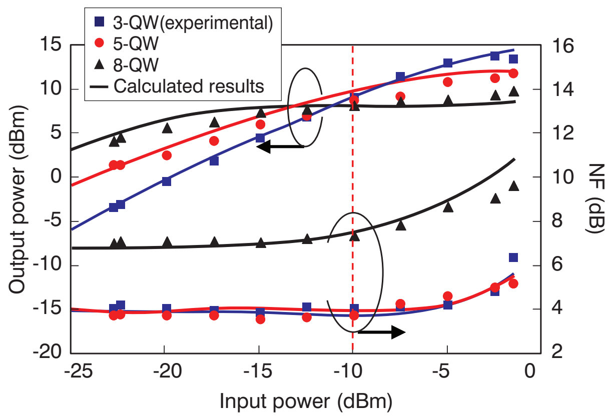

Figure 7 **The output power and the NF characteristics of fabricated SOAs.**

5. CONCLUSION

In this paper, design and prototyping of low-noise SOAs have been conducted through numerical analyses that adopt net gain data actually measured to predict the performance of such SOAs. The SOA of the 5-QW structure prototyped here has raised the prospect of achieving a module NF of 6 dB, which is equivalent to that of erbium doped fiber amplifiers even if a coupling loss of about 2 dB is taken into account. Also, a chip output power of higher than 5 dBm has been achieved, which fully satisfies the performance required for single-channel amplifiers. These results demonstrate that the SOA is promising as a compact, low power consumption and low noise optical amplifier for next-generation optical communications.

REFERENCES

1) T. Sakamoto, A. Chiba and T. Kawanishi, "50-Gb/s 16 QAM by a quad-parallel Mach-Zehnder modulator," European Conference on Optical Communications Conf., Tech. Dig, 2007 paper No. PDS 2.8, (2007)
2) T. Hashimoto, Y. Nakasuga, Y. Yamada, H. Terui, M. Yanagisawa, K. Moriwaki, Y. Suzaki, Y. Tohmori, Y. Sakai, H. Okamoto, "Hybrid integration of spot-size converted laser diode on planar lightwave circuit platform by circuit platform by passive alignment technique," IEEE Photon. Technol. Lett., vol. 8, no. 11, pp. 1504–1506, November 1996.
3) K. Morito, S.Tanaka, S.Tomabechi, and A. Kuramata, "A broad-band MQW semiconductor optical amplifier with high saturation output power and low noise figure," IEEE Photon. Technol. Lett., vol. 17, no. 5, pp. 974–976, May 2005.
4) M. J. Michael, "Wideband Semiconductor Optical Amplifier Steady-State Numerical Model," IEEE J. Quantum Electron, vol. 37, no. 3, pp. 439–447, March 2001.
5) T. Makino, "Analytical formulas for the optical gain of quantum wells," IEEE J. Quantum Electron, vol. 32, no. 3, pp. 493–501, March 1996.
6) B. W. Hakki and T. L. Paoli, "Gain spectra in GaAs double-heterostructure injection lasers," J. Appl. Phys., vol. 46, no. 3, pp. 1299–1306, March 1975.
7) H. Hasegawa, M. Funabashi, N. Yokouchi, K. Kiyota, and K. Maruyama, "Design and Fabrication of Semiconductor Optical Amplifier with Low Noise Figure," OptoElectronics and Communications Conf., Tech. Dig, 2010 paper No. 7D2-3, (2010)